Rotational energy transfer within the B 3Π g v=3 manifold of molecular nitrogen

Ashraf Ali and Paul J. Dagdigian

Citation: The Journal of Chemical Physics **87**, 6915 (1987); doi: 10.1063/1.453386
View online: http://dx.doi.org/10.1063/1.453386
View Table of Contents: http://scitation.aip.org/content/aip/journal/jcp/87/12?ver=pdfcov
Published by the AIP Publishing

Rotational energy transfer within the $B\,^3\Pi_g$ $v=3$ manifold of molecular nitrogen

Ashraf Ali and Paul J. Dagdigian
Department of Chemistry, The Johns Hopkins University, Baltimore, Maryland 21218

(Received 28 July 1987; accepted 2 September 1987)

An optical–optical double resonance experiment has been carried out to study rotationally inelastic collisions of N_2 $B\,^3\Pi_g$ $v=3$ by argon with initial and final state resolution. Nitrogen molecules in the metastable A state are generated by collisional excitation transfer from metastable argon atoms in a flow system. Specific B state rotational levels are prepared by pulsed pump laser excitation of isolated rotational lines in the $B\,^3\Pi_g$–$A\,^3\Sigma_u^+$ (3,0) band near 688 nm. After a short delay, a probe laser interrogates the rotational populations in the B state by fluorescence excitation in the $C\,^3\Pi_u$–$B\,^3\Pi_g$ (0,3) band near 406 nm. Collisional transfer from incident levels in all three spin–orbit manifolds of the B state was investigated. For molecules initially in the F_1 ($\Omega=0$) manifold, a preference for conservation of fine-structure label with even ΔJ changes was observed. This propensity is very pronounced for the $J=0$ level but is considerably relaxed for the higher levels investigated. By contrast, inelastic collisions involving the F_2 ($\Omega=1$) and F_3 ($\Omega=2$) manifolds do not exhibit a significant propensity to conserve fine-structure label. A slight residual preference for even ΔJ changes is observed in collisional transitions within the F_2 manifold. These experimental results are compared to the propensity rules expected for homonuclear $^3\Pi$ rotationally inelastic collisions, both in the case (a) and (b) limits. The reduction of the predicted propensities by the transition to intermediate case coupling and "orbital-correlated" scattering is discussed. The latter term refers to the difference potential for the N_2–Ar interaction when the N_2 unfilled π orbital is in or perpendicular to the triatomic plane. An unsuccessful attempt to detect collisional interelectronic transfer from the B state to the $W\,^3\Delta_u$ state by G–W laser fluorescence excitation is also reported.

I. INTRODUCTION

There has been a long-standing interest in understanding the detailed mechanisms that govern energy flow in systems containing electronically excited nitrogen molecules.[1] Since it is the major component of the Earth's atmosphere, knowledge about collisional processes involving N_2 is crucial for an understanding of phenomena such as auroras and airglows. In the laboratory, nitrogen is often present in gas mixtures in discharges, including various laser gas media. In many discharges, the most prominent electronic transition is the $B\,^3\Pi_g$–$A\,^3\Sigma_u^+$, so-called first positive, band system.[2–4] Since the radiative lifetime of the $B\,^3\Pi_g$ state is 5–10 μs, depending on the vibrational level,[5–7] collisional transitions involving this state are rather significant at the typical pressures of discharges.

Pulsed laser excitation with time-resolved observation of the subsequent B–A fluorescence has been employed in several laboratories[8–10] to obtain information on collisional properties of a range of $N_2(B)$ vibrational levels. In many cases, nonexponential decay of the initially excited vibrational level was observed, indicative of collision-induced transitions to neighboring electronic states. The primary state to which the $B\,^3\Pi_g$ state is collisionally coupled is the nearly isoenergetic[2,11] $W\,^3\Delta_u$ state. The B state also undergoes transitions to the $B'\,^3\Sigma_u^-$ state, as evidenced by B'–B fluorescence emission after laser excitation to the B state.[9(c)] In addition, $A\,^3\Sigma_u^+$ vibrational levels are collisionally coupled to the B and W state manifolds.[9(a),9(d)] These experimental studies were carried out with vibrational, but not rotational, state resolution.

Recently, optical–optical double resonance (OODR) has been employed by Katayama[12] and in our laboratory[13] to study, with initial and final rotational state resolution, collision-induced electronic transitions in CN and N_2^+ between their A and X electronic states. Here we apply this technique to the study of collisional transitions of nitrogen molecules in the $B\,^3\Pi_g$ state. Relative cross sections for pure rotational transitions within the B state are determined by probe laser fluorescence excitation in the C–B band system after B–A pump laser excitation of specific B state rotational levels. The present study is quite similar to a recent investigation of the same process by Katayama.[14] However, our experiment extends his study in that we have determined final state populations from the OODR spectra. In addition, our higher probe and pump laser spectral resolution has allowed a wider range of levels to be studied.

We also report here an unsuccessful attempt to detect N_2 molecules which have undergone collisional transitions from the B to the W state. In this search, we tried to observe $N_2(W)$ molecules by laser fluorescence excitation in the, as yet unreported, $G\,^3\Delta_g$–$W\,^3\Delta_u$ band system. This transition is allowed and involves a $3\sigma_g \leftarrow 1\pi_u$ electron jump. As we discuss below, a possible reason for our lack of success is the near cancellation of the transition moment from the two dominant electron configurations in the description of the G state.

 0021-9606/87/246915-12$02.10

This paper is organized in the following manner: The next section gives a brief description of the apparatus and the bands used for excitation and laser fluorescence probing of the relevant molecular nitrogen rotational levels. Section III gives a review of the collision theory for pure rotational transitions within a $^3\Pi$ state. This treatment extends that of Pouilly and Alexander,[15] who only considered $^3\Pi$ molecules in the case (a) limit. We present here the corresponding results for intermediate and case (b) coupling and derive propensity rules in the case (b) high J limit, to complement those earlier derived by Pouilly and Alexander[15] for case (a) coupling. Section IV A presents and qualitatively discusses our experimental OODR spectra; actual final state populations for each of the incident levels studied are given in Sec. IV B. A detailed description of our unsuccessful search for the $W\,^3\Delta_u$ state is presented in Sec. IV C. A discussion and conclusion follow.

II. APPARATUS

An extensive description of the experimental apparatus and OODR technique employed for the determination of initial- and final-state resolved inelastic cross sections has been given previously in connection with our studies of $A \rightarrow X$ collision-induced electronic transitions in the CN radical.[13] In the present experiments, nitrogen molecules in the metastable $A\,^3\Sigma_u^+$ state are prepared through the $Ar(^3P_{0,2}^0) + N_2$ excitation transfer process[16] in a flow of 3.3 Torr of argon by the addition of a small amount of nitrogen to a flow containing metastable argon atoms, which were produced in a low-current dc hollow-cathode discharge.[1] Thus, the collision partner in these experiments is predominantly argon. The argon carrier gas was purified by passage through liquid-nitrogen cooled molecular sieve traps. While the $Ar(^3P_{0,2}^0) + N_2$ excitation transfer process is known to produce significant N_2 excited-state emission,[16] the estimated flow time of 5 ms between the reagent mixing zone and the pump and probe laser excitation zone allows relaxation of the electronically excited radiating states.

Fluorescence induced by the pump and probe lasers was observed by a photomultiplier (EMI9816 or 9813) perpendicular to the gas flow direction and the laser beams, which were combined on a dichroic mirror. The output of the photomultiplier was converted to a dc signal by a boxcar averager. The pump and probe sources were dye lasers pumped by a Nd:YAG and XeCl laser, respectively; typical dye laser pulse energies were 25 and 2 mJ at a 10 Hz repetition rate. Dye solutions employed in the pump and probe lasers were LDS 680 (Exciton) in methanol and diphenylstilbene in p-dioxane, respectively. The delay between the ~ 10 ns long pump and probe laser pulses was controlled electronically and was typically less than 50 ns.

The $Ar(^3P_{0,2}^0) + N_2$ reaction populates low vibrational levels of the nitrogen A state by radiative cascade from the C and then B states.[16] Individual rotational levels in the $B\,^3\Pi_g$ $v = 3$ manifold were populated by pulsed pump laser irradiation on isolated lines in the first positive B–A (3,0) band[2–4] near 688 nm. Figure 1 displays a pump laser fluorescence excitation spectrum of this band. It can be seen that there is extensive overlapping of rotational lines. For a transition between a $^3\Sigma$ and $^3\Pi$ state, there are 27 allowed rotational branches, and all of these have appreciable intensity when the $^3\Pi$ state coupling is near Hund's case (a) and the $^3\Sigma$ state is well described by case (b) coupling,[17] as is the case for the $A\,^3\Sigma_u^+$ and $B\,^3\Pi_g$ states of molecular nitrogen.[2–4] Nevertheless, at our ~ 0.3 cm^{-1} effective resolution, a reasonable number of B state rotational levels can be individually excited in all three spin–orbit manifolds, although the available number is greatest for the F_1 manifold.

Both the initially excited and collisionally populated rotational levels were monitored by laser fluorescence detection of C–B (0,0) band emission through a UV filter (340 center wavelength, 10 nm bandpass) upon probe laser excitation in the second positive $C\,^3\Pi_u$–$B\,^3\Pi_g$ (0,3) band near 406 nm.[2] Individual lines in the OODR spectra were identified with the help of a spectral atlas.[3] Even though the C–B (0,3) band has a Franck-Condon factor of only 0.0517,[2] spectra were obtained with very good signal-to-noise ratio. The E vector for both pump and probe lasers was in the plane defined by the axis of the laser beams and the photomultiplier.

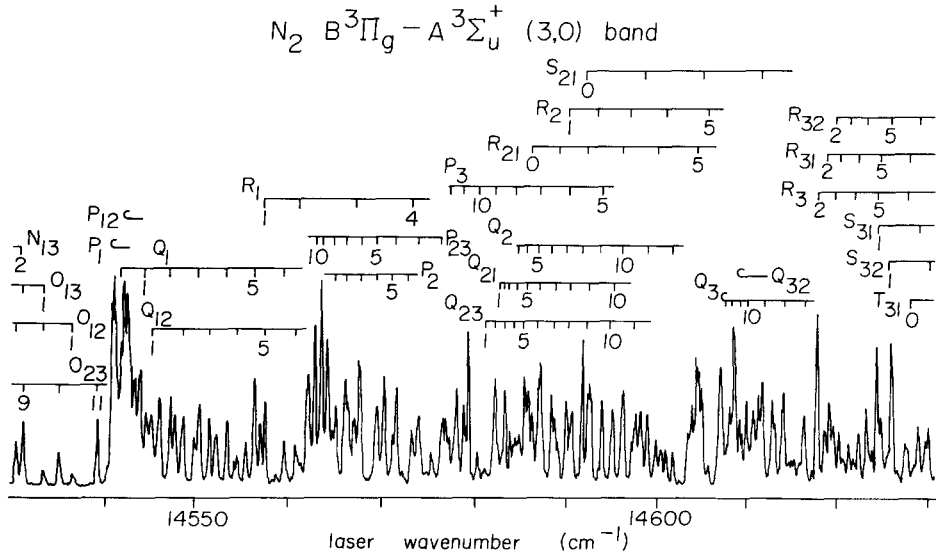

FIG. 1. Pump laser fluorescence excitation spectrum of the N_2 $B\,^3\Pi_g$–$A\,^3\Sigma_u^+$ (3,0) band. Lines of the various rotational branches [in case (b) notation] are indicated, and individual lines are identified by the quantum number N for the lower state.

III. REVIEW OF COLLISION THEORY FOR $^3\Pi$ MOLECULES

Pouilly and Alexander[15] have considered the quantum collision dynamics for rotationally inelastic collisions involving molecules in $^3\Pi$ electronic states and have derived matrix elements of the interaction potential in a case (a) basis. We review their results here and extend their treatment to intermediate case coupling. We also present their derived propensity rules, as well as similar predictions for the case (b) high-J limit.

The wave function for a diatomic molecule in a definite-parity case (a) basis can be written as[18–20]

$$|JM\Omega v S\epsilon\rangle = 2^{-1/2}[\,|JM\Omega\rangle|vS\Lambda\Sigma\rangle + \epsilon|JM,-\Omega\rangle|vS,-\Lambda,-\Sigma\rangle\,]\,, \tag{1}$$

where $\epsilon = \pm 1$, and J denotes the total angular momentum, with space- and body-fixed projections M and Ω, respectively; S and Σ are the electronic spin angular momentum and its body-fixed projection; and Λ and v are the body-fixed projection of the electronic orbital angular momentum and the vibrational quantum number. The total parity[21] of the wave function $|JM\Omega vS\epsilon\rangle$ in Eq. (1) is $\epsilon(-1)^{J-1}$ so that levels with $\epsilon = -1$ are labeled in modern spectroscopic notation[22] as **e**, and $\epsilon = +1$ as **f**. For homonuclear diatomics, the rotational levels can be classified by their permutation-inversion symmetry.[18] For a *gerade* Π electronic state, as, e.g., the $B\,^3\Pi_g$ state of N_2, the even-parity states $[\epsilon(-1)^{J-1} = +1]$ are symmetric with respect to this operation and are labeled **s**, while the odd-parity states $[\epsilon(-1)^{J-1} = -1]$ are antisymmetric and are labeled **a**.

The molecular eigenfunctions of a given J are traditionally labeled F_1, F_2, and F_3 in order of increasing energy.[17] The case (a) basis functions given in Eq. (1) are molecular eigenfunctions only if the spin–orbit splitting $A\,\mathbf{L}\cdot\mathbf{S}$ is much larger than BJ. In the case (a) limit, we have $\Omega = 0$, 1, and 2 for the F_1, F_2, and F_3 levels, respectively, for $A > 0$, as is true for $N_2(B)$.[2] However, since $A/B = 25.8$ for $N_2(B)$,[2] a coupling scheme intermediate between Hund's cases (a) and (b) is more appropriate for the J values accessed in the present experiments ($J \leqslant 16$). We can express the eigenfunctions as follows:

$$|JMF_i\epsilon\rangle = \sum_{\Omega=0}^{2} C^{\Omega}_{JF_i\epsilon}|JM\Omega\epsilon\rangle\,. \tag{2}$$

For simplicity, we have suppressed the labels S and v in Eq. (2). The matrix elements of the rotational + spin–orbit Hamiltonian are given in Table I.[18,20,23] In the absence of Λ doubling, this matrix is independent of the symmetry index ϵ, so that the coefficients $C^{\Omega}_{JF_i\epsilon}$ in Eq. (2) would also be the same for $\epsilon = \pm 1$. In the case (b) limit, where $BJ \gg A$, the expansion coefficients are given by[23]

$$C^{\Omega}_{JF_i\epsilon} = (-1)^{N-J+\Sigma}(JS\Omega - \Sigma|N\Lambda)\,, \tag{3}$$

where $(\cdots|\cdot\cdot)$ is a Clebsch–Gordan coefficient.[24] The quantum number N represents the angular momentum excluding electron spin and equals $J-1$, J, and $J+1$ for the F_1, F_2, and F_3 levels, respectively. The rotational energies in the $v = 3$ manifold of the N_2 $B\,^3\Pi_u$ electronic state are displayed in Fig. 2.

TABLE I. The rotational + spin–orbit Hamiltonian in a case (a) basis.[a]

	$H_{\Omega'\Omega}$		
Ω'	$\Omega = 0$	1	2
0	$B(x+1) - A$	$-\sqrt{2x}B$	0
1	$-\sqrt{2x}B$	$B(x+1)$	$-\sqrt{2x-4}B$
2	0	$-\sqrt{2x-4}B$	$B(x-3) + A$

[a] Reference 20. Centrifugal effects and Λ doubling ignored here. The quantity x is defined as $J(J+1)$. The rotational constant B and spin–orbit parameter A are those appropriate to the vibrational level under consideration.

For high J, the Clebsch–Gordan coefficients in Eq. (3) approach limiting values, and the molecular eigenfunctions in this limit equal

$$|JMF_1\epsilon\rangle = 2^{-1}[\,|JM,\Omega=0,\epsilon\rangle + |JM,\Omega=2,\epsilon\rangle\,] + 2^{-1/2}|JM,\Omega=1,\epsilon\rangle\,, \tag{4a}$$

$$|JMF_2\epsilon\rangle = 2^{-1/2}[\,|JM,\Omega=0,\epsilon\rangle - |JM,\Omega=2,\epsilon\rangle\,]\,, \tag{4b}$$

$$|JMF_3\epsilon\rangle = 2^{-1}[\,|JM,\Omega=0,\epsilon\rangle + |JM,\Omega=2,\epsilon\rangle\,] - 2^{-1/2}|JM,\Omega=1,\epsilon\rangle\,. \tag{4c}$$

We see that the contribution of the different Ω basis functions to a given eigenfunction varies significantly between the case (a) and (b) limits. This variation is most pronounced for the F_2 level: In case (a), this eigenfunction is composed exclusively of $\Omega = 1$, while in the opposite case (b) limit, Eq. (4b) shows that it is an equal admixture of $\Omega = 0$ and 2. This behavior has significant implications for the electronic symmetry[25] of $^3\Pi$ Λ doublet levels.[26]

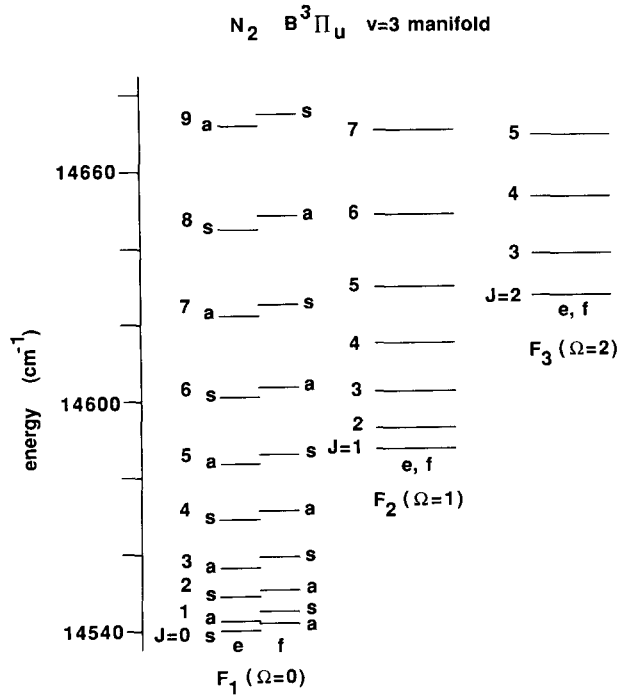

FIG. 2. Rotational energies (referred to the lowest level of the $A\,^3\Sigma_u^+$ electronic state) of the $v = 3$ manifold of the N_2 $B\,^3\Pi_g$ state. The Λ doubling in the F_2 and F_3 manifolds is too small to be shown in the figure.

The approach of a spherical atomic scattering partner, such as argon, removes the twofold degeneracy of the Π diatomic molecular state and produces two potential energy surfaces, one symmetric (A') and another antisymmetric (A'') with respect to reflection of the electronic spatial coordinates in the triatomic plane.[27] The most common electron occupancies for $^3\Pi$ electronic states are $\sigma\pi$ or $\sigma\pi^3$.[17] The A' and A'' surfaces correspond to having the π electron (or hole) in or perpendicular to the molecular plane, respectively. These surfaces, which are functions of the distance R between the molecular center of mass and the collision partner and the angle β between the molecular bond axis and the z axis of the triatomic body-fixed frame, are denoted V_+ and V_-, respectively. The wave function for the composite system consisting of the molecule and structureless scattering partner can be expressed as linear combination of products of molecular eigenfunctions [Eq. (2)] and wave functions describing the relative orbital motion of the collision system.[28] It is convenient to choose the wave functions for the total system to be eigenfunctions of the total angular momentum J. Matrix elements of the interaction potential in this $|JF_i\epsilon L\mathscr{J}\mathscr{M}\rangle$ basis, which are required for solution of the close-coupled (CC) equations,[29] have been presented previously by Pouilly and Alexander[15] in the case (a) molecular basis. For intermediate coupling [Eq. (2)] in a $^3\Pi$ state, these matrix elements can be written as

$$\langle {}^3\Pi J'F_i'\epsilon' L'\mathscr{J}\mathscr{M}|V|{}^3\Pi JF_i\epsilon L\mathscr{J}\mathscr{M}\rangle = (-1)^{J+J'+\mathscr{J}}[(2L+1)(2L'+1)(2J+1)(2J'+1)]^{1/2} \times \sum_l \begin{pmatrix} L' & l & L \\ 0 & 0 & 0 \end{pmatrix} \begin{Bmatrix} J' & L' & \mathscr{J} \\ L & J & l \end{Bmatrix} \frac{1}{2}[1+\epsilon\epsilon'(-1)^{J+J'+l}] \times \left[A^l_{J'F_i'\epsilon',JF_i\epsilon} V_{l0}(R) + B^l_{J'F_i'\epsilon',JF_i\epsilon} V_{l2}(R)\right], \tag{5}$$

where

$$A^l_{J'F_i'\epsilon',JF_i\epsilon} = \sum_{\Omega=0}^{2} (-1)^{\Omega} C^{\Omega}_{J'F_i'\epsilon'} C^{\Omega}_{JF_i\epsilon} \begin{pmatrix} J' & l & J \\ -\Omega & 0 & \Omega \end{pmatrix}, \tag{6a}$$

$$B^l_{J'F_i'\epsilon',JF_i\epsilon} = \epsilon \sum_{\Omega=0}^{2} (-1)^{\Omega} C^{2-\Omega}_{J'F_i'\epsilon'} C^{\Omega}_{JF_i\epsilon} \begin{pmatrix} J' & l & J \\ \Omega-2 & 2 & -\Omega \end{pmatrix}. \tag{6b}$$

The radial terms $V_{l0}(R)$ and $V_{l2}(R)$ are coefficients in the expansion of the sum $V_{\rm sum}$ and difference $V_{\rm diff}$, respectively, of V_+ and V_- in terms of the Legendre and associated Legendre polynomials $P_l(\cos\beta)$ and $P^2_l(\cos\beta)$.[27]

From an examination of the matrix element of V in the case (a) limit, Pouilly and Alexander[15] have derived several selection rules for rotationally inelastic collisions in a $^3\Pi$ electronic state. Firstly, collisional transitions between the $^3\Pi_1$ and $^3\Pi_0$ or $^3\Pi_2$ fine-structure manifolds will be rigorously forbidden. This rule is related to the fact that the molecule-fixed projection Σ of the electron spin cannot be changed by the purely electrostatic forces in a collision; $^3\Pi_1$ levels have $\Sigma = 0$, while $^3\Pi_0$ and $^3\Pi_2$ levels involve $\Sigma = \pm 1$ [see Eq. (1)]. In addition, collisional change of the **e/f** symmetry label will not be allowed for transitions within the $^3\Pi_0$ manifold. Finally, asymmetries in the magnitudes of the cross sections for upward ($+\Delta J$) and downward ($-\Delta J$) transitions will be manifest within the $^3\Pi_1$ manifold, as has already been documented for transitions within a $^1\Pi$ state.[30–33] These general rules do not depend on the applicability of a particular dynamical limit or form of the interaction potential but only require that the molecular eigenfunctions be in the case (a) limit. In addition, there will be other, more restrictive, propensity rules which are common to all open-shell case (a) diatomic electronic states, e.g., conservation of **e/f** symmetry within all fine-structure manifolds at high J whenever a Born or infinite-order sudden approximation applies to the collision dynamics.[15,28,34–36]

In the case of a homonuclear diatomic such as N_2, only the even l terms $V_{l0}(R)$ and $V_{l2}(R)$ in Eq. (5) are nonzero. The vanishing of the odd l coefficients through the phase factor following the $6j$ symbol in Eq. (5) leads to the exclusion of collisional transitions between **s** and **a** levels.[12,37] In the case of the $^3\Pi_0$ manifold, this conservation of nuclear permutation symmetry and of **e/f** symmetry derived by Pouilly and Alexander[15] implies that only even ΔJ transitions will have nonzero couplings in the case (a) limit (see Fig. 2). This selection rule is entirely analogous to the known prohibition of odd ΔJ collisional transitions for a homonuclear $^1\Sigma$ molecule.[38] In a real $^3\Pi$ state, such as N_2 $B\,^3\Pi_g$, the transition to intermediate, and then case (b), coupling as J increases will induce a breakdown in these derived selection rules. As we shall see below, the most important mechanism for this breakdown involves the difference potential $V_{\rm diff}$. We note that the matrix element in Eq. (5) will still remain zero for odd ΔJ transitions from the $J = 0$ F_1 **e** or **f** levels since these rigorously can have no $\Omega = 1$ or 2 admixture.

It is interesting to investigate the form of the matrix elements in Eq. (5) for the interaction potential in the case (b), high-J limit. First we substitute in Eq. (5) the limiting form of the mixing coefficients $C^{\Omega}_{JF_i\epsilon}$ given by Eq. (4) and utilize the semiclassical limit of the $3j$ symbol appearing in Eq. (6a). For $J, J' \gg l$, this $3j$ symbol can be approximated[36] as

$$\begin{pmatrix} J' & l & J \\ -\Omega & 0 & \Omega \end{pmatrix} = (-1)^{\Omega} \cos(\Omega\omega_{12}) \begin{pmatrix} J' & l & J \\ 0 & 0 & 0 \end{pmatrix} \tag{7}$$

for $J' + l + J$ even. (This $3j$ symbol goes to zero as J and J' become large for $J' + l + J$ odd.[36]) Here ω_{12} is the angle between the classical angular momentum vectors **j** and **j'** and

is small in this limit. We thus find that the last term in square brackets in Eq. (5) can be written as

$$V_{l0}(R)\begin{pmatrix} J' & l & J \\ 0 & 0 & 0 \end{pmatrix} + \epsilon V_{l2}(R)\left[a\begin{pmatrix} J' & l & J \\ -2 & 2 & 0 \end{pmatrix} + b\begin{pmatrix} J' & l & J \\ -1 & 2 & -1 \end{pmatrix} + c\begin{pmatrix} J' & l & J \\ 0 & 2 & -2 \end{pmatrix}\right] \quad (8)$$

For F_i-conserving transitions, where $a = 1/4$, $b = -1/2$, $c = 1/4$ for the F_1 and F_3 manifolds, and $a = c = -1/2$, $b = 0$ for the F_2 manifold. For F_i-changing transitions, this term is given by

$$2^{-3/2}\epsilon V_{l2}(R)\left[\begin{pmatrix} J' & l & J \\ 0 & 2 & -2 \end{pmatrix} - \begin{pmatrix} J' & l & J \\ -2 & 2 & 0 \end{pmatrix}\right] \quad \text{for } F_1 \to F_2,\ F_2 \to F_3\,, \quad (9a)$$

$$4^{-1}\epsilon V_{l2}(R)\left[\begin{pmatrix} J' & l & J \\ 0 & 2 & -2 \end{pmatrix} + 2\begin{pmatrix} J' & l & J \\ -1 & 2 & -1 \end{pmatrix} + \begin{pmatrix} J' & l & J \\ -2 & 2 & 0 \end{pmatrix}\right] \quad \text{for } F_1 \to F_3\,. \quad (9b)$$

Equations (8) and (9) may be further simplified by utilizing a standard recursion relation.[39] We have

$$[(J-1)(J+2)]^{1/2}\begin{pmatrix} J' & l & J \\ 0 & 2 & -2 \end{pmatrix} + [J'(J'+1)]^{1/2}\begin{pmatrix} J' & l & J \\ -1 & 2 & -1 \end{pmatrix} + [(l-1)(l+2)]^{1/2}\begin{pmatrix} J' & l & J \\ 0 & 1 & -1 \end{pmatrix} = 0 \quad (10a)$$

and

$$[J(J+1)]^{1/2}\begin{pmatrix} J' & l & J \\ -2 & 2 & 0 \end{pmatrix} + [(J'-1)(J'+2)]^{1/2}\begin{pmatrix} J' & l & J \\ -1 & 2 & -1 \end{pmatrix} + [(l-2)(l+3)]^{1/2}\begin{pmatrix} J' & l & J \\ -2 & 3 & -1 \end{pmatrix} = 0\,. \quad (10b)$$

Hence, one can show from Eqs. (10a) and (10b) that for $J, J' \gg l$,

$$\begin{pmatrix} J' & l & J \\ 0 & 2 & -2 \end{pmatrix} \approx \begin{pmatrix} J' & l & J \\ -2 & 2 & 0 \end{pmatrix} \approx -\begin{pmatrix} J' & l & J \\ -1 & 2 & -1 \end{pmatrix}. \quad (11)$$

For large initial and final angular momenta, the terms multiplying $V_{l2}(R)$ in Eqs. (9a) and (9b) will thus approach zero for fine-structure-changing transitions. In addition, we see that for fine-structure-conserving transitions Eq. (8) becomes

$$V_{l0}(R)\begin{pmatrix} J' & l & J \\ 0 & 0 & 0 \end{pmatrix} + \epsilon V_{l2}(R)\begin{pmatrix} J' & l & J \\ -2 & 2 & 0 \end{pmatrix}. \quad (12)$$

Hence, we find that in the case (b) high-J limit only fine-structure-conserving transitions will be allowed. This result was also derived for collisions of case (b) $^2\Pi$ molecules in the high-J limit.[28] This derived conservation of fine-structure level is formally equivalent to the prediction[34,36,40] and experimental demonstration[41,42] of a similar conservation rule for transitions within $^{2S+1}\Sigma$ electronic states in collisions with structureless targets. In both $^{2S+1}\Sigma$ and case (b) Π electronic states, the different fine-structure levels F_i correspond to different vector coupling of **J** and **S** to form **N**. This collisional propensity rule merely restates the physical property that in a collisional interaction with only electrostatic forces operative, the direction of the electronic spin **S** cannot be changed so that the angle between **N** and **J** will not be altered.

It is important to note that this fine-structure conservation rule for $^3\Pi$ collisions is, strictly speaking, only valid in the high-J limit. Numerical calculation of the coefficients $B^l_{J'F_i'\epsilon',JF_i\epsilon}$ multiplying the terms V_{l2} in the difference potential approach zero asymptotically as a function of increasing J. The asymptotic limits for the $3j$ symbols given in Eqs. (7) and (11) as J and J' become large are reached increasingly slowly for larger Ω values, as can be seen, for example, from Eq. (7).

Equation (12) shows that in the case (b) high-J limit both the sum and difference potentials $V_{\rm sum}$ and $V_{\rm diff}$ play a role in inducing fine-structure conserving collisional transitions, as has already been shown for $^2\Pi$(b) collisions.[28] This implies, e.g., that the even ΔJ selection rule derived previously[15] for homonuclear $^3\Pi$(a) collisions within the $\Omega = 0$ manifold can be significantly violated as J increases since the $3j$ symbol multiplying the V_{l2} term in Eq. (1) does not go to zero for $J' + l + J$ odd, as does the first $3j$ symbol in this equation.[24] (Recall that for a homonuclear molecule only the even l V_{l0} and V_{l2} terms can be nonzero for a homonuclear molecule.) Figure 3 shows, e.g., that for N_2 $B\,^3\Pi_g$ collisions within the F_1 manifold for $J \leqslant 30$, the $B^l_{J'F_i'\epsilon',JF_i\epsilon}$ coefficients for odd ΔJ transitions become comparable in magnitude to the $A^l_{J'F_i'\epsilon',JF_i\epsilon}$ coefficient for the corresponding even ΔJ transition as J becomes large; we have set $l = 2$ here since this is the first nonzero value for l in collisions involving a homonuclear molecule. Thus, this even ΔJ propensity rule for F_1 levels will not hold into intermediate case coupling if $V_{\rm diff}$ cannot be neglected in comparison with $V_{\rm sum}$.

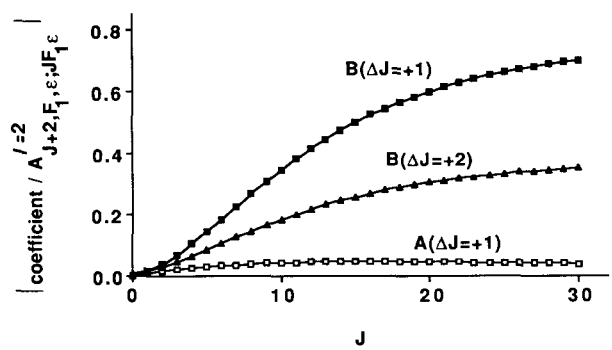

FIG. 3. Calculated values of the absolute values of the coefficients $A^l_{J+1,F_i,-\epsilon;JF_i\epsilon}$ and $B^l_{J'F_i\epsilon',JF_i\epsilon}$ for $\Delta J = J' - J = +1$ and $+2$ to the coefficient $A^l_{J+2,F_i,\epsilon;JF_i\epsilon}$ [see Eqs. (6a) and (6b)] for transitions within the N_2 $B\,^3\Pi_g$ $v = 3$ F_1 manifold. We have set $l = 2$ here. Because of the phase factor in Eq. (5), we must have $\epsilon = \epsilon'$ for even ΔJ and $\epsilon = -\epsilon'$ for odd ΔJ.

It is interesting to compare these derived propensity rules with those for collisions of $^{2S+1}\Sigma$ electronic states with open-shell targets. In this case, the electrostatic intermolecular potential will, in general, vary with the total spin of the composite molecule-target system.[43] The state-resolved inelastic cross sections in this case can be expressed as a sum of a spin-independent and spin-correlated cross section.[44] For a $^2\Sigma$ molecule–^2S atom collision, the former is a degeneracy weighted sum of squares of T-matrix elements for scattering on the composite-system singlet and triplet surfaces, while the latter involves squares of the differences of these elements. The spin-independent term predicts the same propensity for collisional fine-structure conservation as with a structureless target, while no such propensity is present for the spin-correlated term. Thus, if the difference between the singlet and triplet potentials is large enough, this propensity rule will be violated for a $^2\Sigma$–^2S interaction. A large singlet–triplet separation would be expected if a strong chemical bond could be formed between the collision partners, leading to a large exchange interaction.

Equations (5) and (6) suggest that the potentials $V_{\rm sum}$ and $V_{\rm diff}$ play the same role as the sum and difference of the singlet and triplet spin multiplicity potentials in $^2\Sigma$–^2S collisions. Thus, the propensity for conservation of the fine-structure label will be lost if orbital-correlated scattering due to $V_{\rm diff}$ is important. This would be the case, e.g., if the presence or absence of the unpaired π electron (or hole) in the scattering plane would significantly change the mainly repulsive interaction (at 300 K thermal collision energies) between the $^3\Pi$ molecule and a closed-shell target, such as an inert gas atom.

IV. RESULTS

A. Double resonance spectra

Double resonance spectra of the C–B (0,3) band were obtained for small pump–probe delays for a range of initially excited rotational levels in all three spin–orbit manifolds of $B\,^3\Pi_g$ $v=3$. Typical pump–probe delays were 10–20 ns; multiple collision effects became evident for delays greater than 50 ns. Figures 4–7 present such spectra for four different initial levels. Since the $C\,^3\Pi_u$–$B\,^3\Pi_g$ band system is a parallel transition with $\Delta\Lambda=0$, the Q branches will be weak.[17] There are, in fact, only six strong branches, namely P and R branches involving fine-structure-conserving radiative transitions between the two $^3\Pi$ states. In addition, the Q_2 and Q_3 branches have appreciable intensity for small J values. (The Q_1 branch is forbidden since $\Delta J=0$ is not allowed when $\Omega=0$.) Since the upper and lower states have $\Lambda=1$, each rotational level consists of a *pair* of Λ doublet levels, of opposite **e/f** and **s/a** symmetries. As a result, each rotational line is in fact a closely spaced doublet.[17] Because the Λ doubling is largest in the F_1, or $\Omega=0$, manifold[17] (see Fig. 2), this splitting is significant ($\sim$0.3 cm^{-1}) for F_1 branches[3] and is resolvable in the R_1 branch in our OODR spectra.

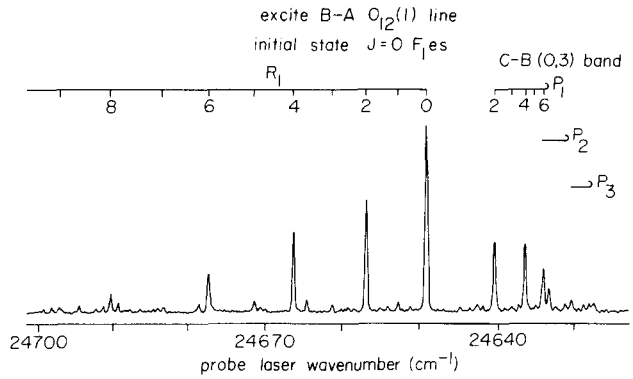

FIG. 4. OODR spectrum of the N_2 $C\,^3\Pi_u$–$B\,^3\Pi_g$ (0,3) band with the pump laser tuned to the $O_{21}(1)$ line of the B–A (3,0) band so as to excite the $v_B=3$ $J=0$ F_1 **es** level. Individual rotational lines of the R_1 and P_1 branches are denoted by the lower state quantum number J. Weak unidentified features are due to excitation in other branches (see succeeding figures). The pump–probe delay was 10 ns.

Figures 4 and 5 display spectra when the $J=0$ and $J=6$ levels of **es** symmetry in the F_1 fine-structure manifold are initially excited. Our spectrum for excitation of $J=0$ is very similar to that previously obtained by Katayama[14] but

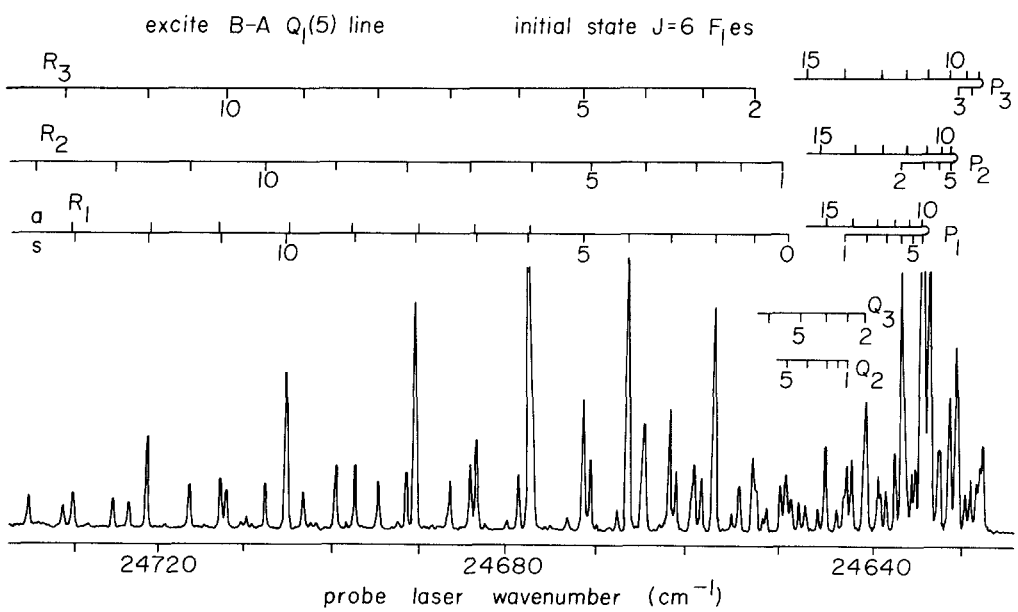

FIG. 5. OODR spectrum of the N_2 $C\,^3\Pi_u$–$B\,^3\Pi_g$ (0,3) band with the pump laser tuned to the $Q_1(5)$ B–A (3,0) line [$J=6$ F_1 **es** level excited]. Individual rotational lines are identified by the lower state quantum number J. The Λ doubling in the R_1 branch is resolvable in the spectrum, and the **s** and **a** symmetries for the individual lines are given. The $R_1(6)$ and $P_1(6)$ parent lines are off scale. The pump–probe delay was 10 ns.

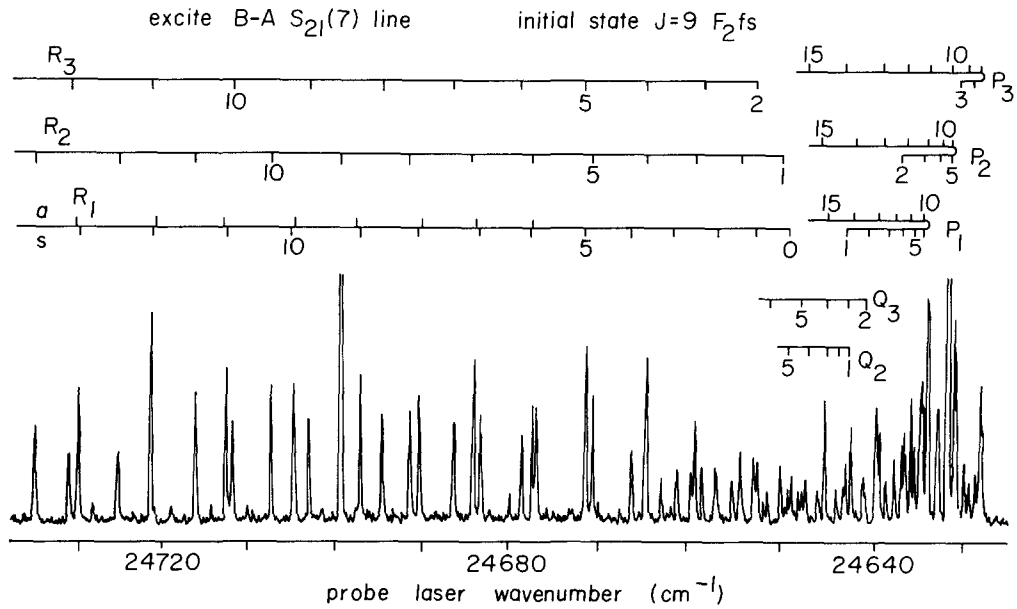

FIG. 6. OODR spectrum of the N_2 $C\,^3\Pi_u$–$B\,^3\Pi_g$ (0,3) band with the pump laser tuned to the $S_{21}(7)$ *B–A* (3,0) line [$J = 9$ F_2 **fs** level excited]. The pump–probe delay was 10 ns.

has significantly higher probe laser spectral resolution. It can be seen from Fig. 4 that inelastic collisions involve almost entirely even ΔJ changes within the F_1 manifold, as earlier noted by Katayama.[14] This even ΔJ propensity rule was anticipated by the general analysis of inelastic collisions of $^3\Pi$ molecules given in Sec. III. Also evident in our spectrum is the presence of weak features which correspond to transitions into the F_2 and F_3 manifolds, as well as to odd ΔJ fine-structure-conserving transitions.

Figure 5 shows that this propensity for even ΔJ changes within the F_1 manifold also occurs for initial $J > 0$, in this case $J = 6$. However, it is also evident that odd ΔJ and fine-structure-changing transitions are considerably more probable than for $J = 0$. A similar observation was made by Katayama[14] in a comparison of OODR spectra for the $J = 5$ vs $J = 0$ initial levels. Figures 6 and 7 present typical spectra for excitation of initial levels in the F_2 and F_3 manifolds, respectively. Unfortunately, population of the $J = 4$ F_3 **fa** level by pump laser excitation of the $T_{31}(2)$ *B–A* line in Fig. 7 also excited a high-J level because of a previously unsuspected overlapping with the $Q_3(20)$ line. Since large ΔJ changes in a single collision are improbable, the presence of these high-J molecules can be ignored so long as we restrict ourselves to the determination of small or intermediate ΔJ transitions from $J = 4$. For the initial levels probed in Figs. 6 and 7, as with our levels investigated in these manifolds, there is little evidence of any propensity to conserve fine-structure manifold in a collision-induced transition. Moreover, in contrast to F_1 initial levels, there is no obvious propensity for even ΔJ transitions within the initially excited fine-structure manifold.

Careful examination of the lines in the R_1 branch of the OODR spectra displayed in Figs. 5–7 reveals small but significant shifts in the wavelengths of these lines with respect

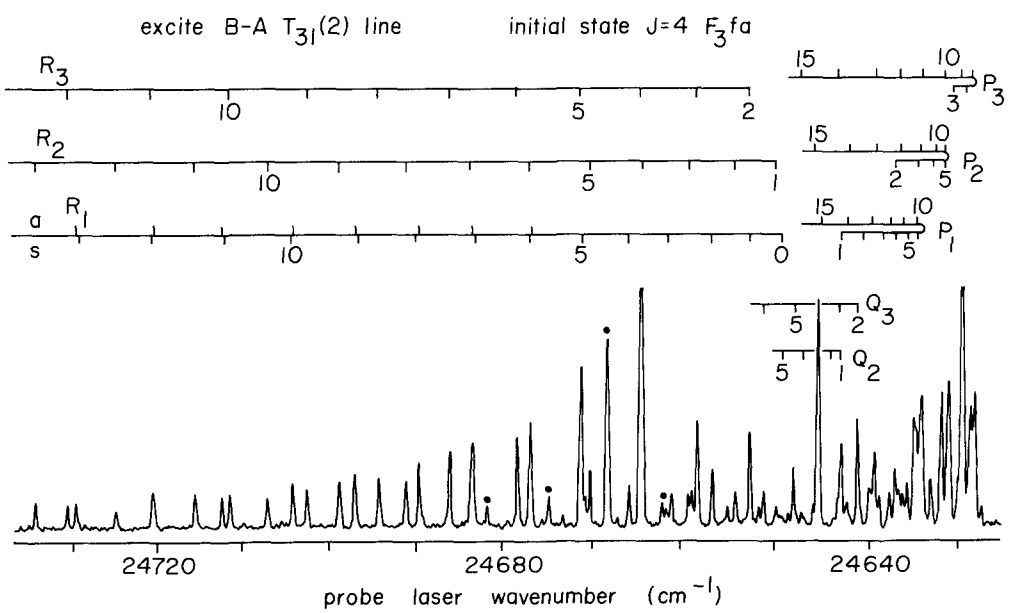

FIG. 7. OODR spectrum of the N_2 $C\,^3\Pi_u$–$B\,^3\Pi_g$ (0,3) band with the pump laser tuned to the $T_{31}(2)$ *B–A* (3,0) line [$J = 4$ F_3 **fa** level excited]. The lines marked with dots are due to excitation of and collisional transfer from the $J = 19$ F_3 **ea** level which is excited by the $Q_3(20)$ *B–A* (3,0) line. This line, which is not listed in the spectral atlas of Dieke and Heath (Ref. 3), unfortunately overlaps the $T_{31}(2)$ line. The pump–probe delay was 10 ns.

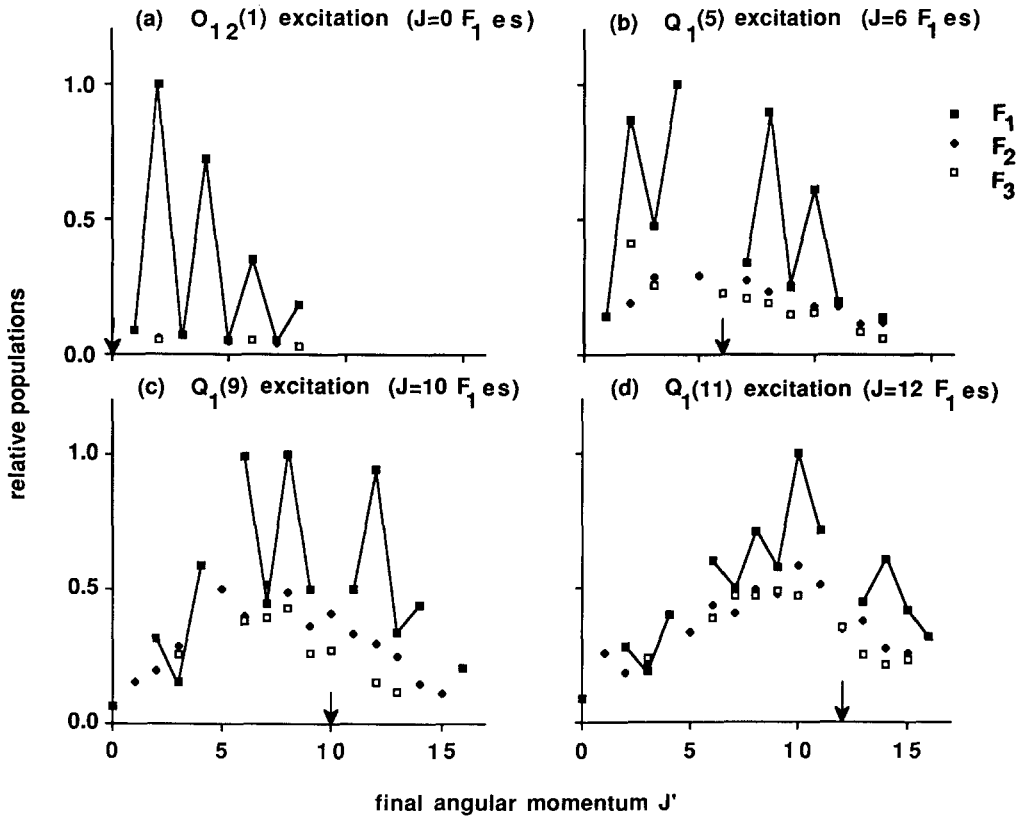

FIG. 8. Final state populations when levels in the F_1 manifold are initially prepared. The *B–A* lines employed for excitation, as well as the identity of the incident levels excited, are given. Each distribution is separately normalized to unity for the most probable level. Final levels in the F_1, F_2, and F_3 manifolds are indicated by solid squares, diamonds, and open squares, respectively. For clarity of viewing, populations in the initial fine-structure manifold are connected with solid lines.

to neighboring lines of other branches. This is particularly obvious for the $R_1(7)$ and $R_2(7)$ lines. In Figs. 5 and 6 these lines are clearly resolved but are overlapped in Fig. 7. The initial *B* state levels excited for the spectra in the former two figures have **s** nuclear permutation symmetry, while the initial state corresponding to the latter has **a** symmetry. As discussed above, the Λ doubling in the F_1 manifold is sufficiently large to cause an observable splitting of the $R_1(7)$ **s** and **a** lines. It is found that the **a** component of this line nearly overlaps the $R_2(7)$ line, while the **s** component is shifted to the red.[3,4] Thus, regardless of the nuclear permutation symmetry of the initial level, only one component of the $R_1(7)$ line, namely the one with the same symmetry as the initial level, is found to have significant intensity. This selective population of a final state with nuclear permutation symmetry identical to that of the initially excited level thus illustrates this expected selection rule for collisions of a homonuclear diatomic molecule.[12,37] In analyzing our spectra, we thus ignore the overlapping of **s** and **a** components of a given line and assume the presence of only the one corresponding to the incident state symmetry. It is interesting to note that the R_1 lines appear as resolved doublets when a *B–A* bandhead is excited (OODR spectrum not shown here) so that a number of *B* state levels, of both **s** and **a** symmetry, are excited.

B. Final state populations

The observed relative intensities of resolved rotational lines in OODR spectra such as those displayed in Figs. 4–7 were used to determine the relative populations in the final rotational states. The relationship of laser-induced fluorescence intensity to rotational populations has been discussed in detail for a general molecule by Greene and Zare.[45] The fluorescence intensity I for excitation of a line in the *C–B* band system from a state of total angular momentum J to an excited state of J' is given by their Eq. (13).[45] The rotational line strength S_a for absorption, which enters this formula, is given for this parallel band system by

$$S = (2J+1)(2J'+1) \times \left| \sum_{\Omega=0}^{2} (-1)^{\Omega} C^{\Omega}_{J'F'_i\epsilon'} C^{\Omega}_{JF_i\epsilon} \begin{pmatrix} J' & 1 & J \\ -\Omega & 0 & \Omega \end{pmatrix} \right|^2, \quad (13)$$

where $C^{\Omega}_{JF_i\epsilon}$ and $C^{\Omega}_{J'F'_i\epsilon'}$ are the mixing coefficients in Eq. (2) for the *B* and *C* state, respectively. A corresponding expression can be written for the emission line strength S_d. We note that because of the parity selection rule on electric dipole transitions, $\epsilon' = \epsilon$ for *P* and *R* branches and $\epsilon' = -\epsilon$ for *Q* branches.

The final state population distributions in the *B* state were determined for a range of incident levels in all three spin–orbit manifolds, using the fluorescence intensity factors described above. For each incident level, the line intensities were taken from an average of several OODR spectra. The derived populations are displayed in Figs. 8, 9, and 10 for incident levels in the F_1, F_2, and F_3 fine-structure manifolds, respectively.

The propensity toward even ΔJ fine-structure-conserving collisional transitions is particularly evident from Fig. 8 for F_1 incident levels. This is expected from the fact that the coupling matrix element V in Eq. (5) vanishes[15] for odd ΔJ transitions in collisions of a homonuclear molecule in case

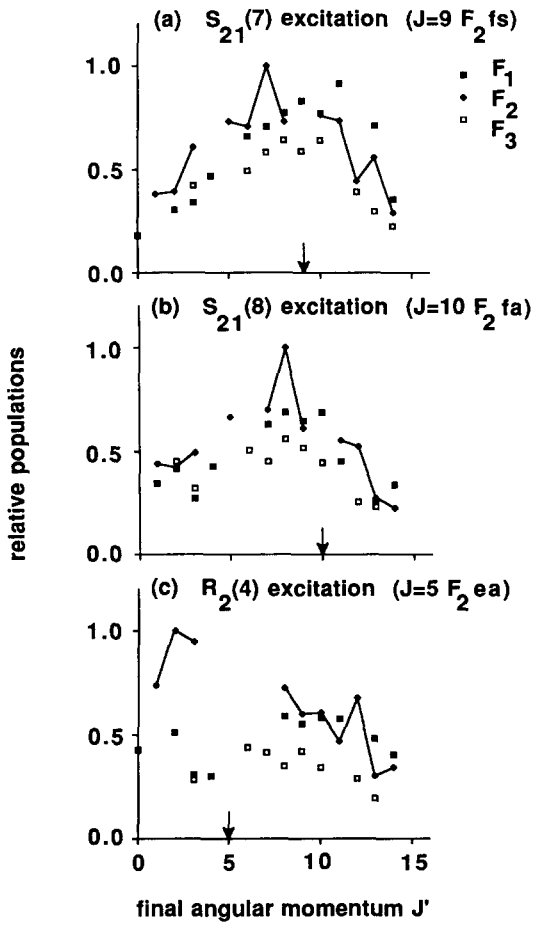

FIG. 9. Final state populations when levels in the F_2 manifold are initially prepared.

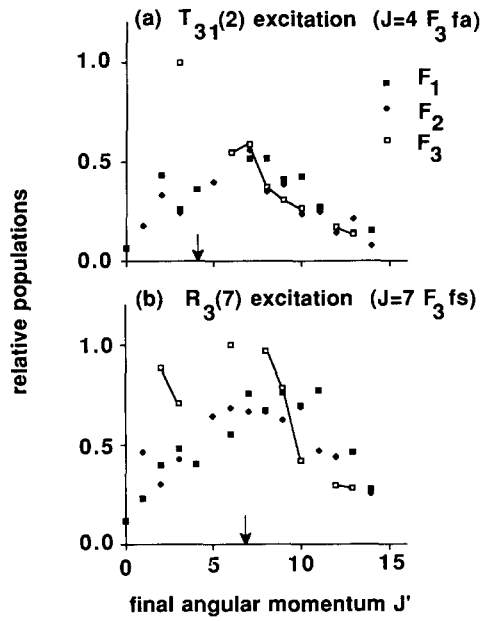

FIG. 10. Final state populations when levels in the F_3 manifold are initially prepared.

(a) coupling. Figure 8(a) shows that the cross sections for odd ΔJ transitions from the incident $J=0$ level are less than 10% of those for even ΔJ. It can be seen from Figs. 8(b) through 8(d) that the amplitude of this even–odd oscillation decreases monotonically as the angular momentum J of the initial level increases. For $J=12$, the populations of final levels for odd ΔJ transitions has grown to 60%–70% of those for even ΔJ. These results suggest that, along with the sum potential $V_{\rm sum}$ the difference potential $V_{\rm diff}$ plays a significant role in inducing inelastic transitions in $N_2(B)$–Ar collisions. Figure 3 indicates that the potential coupling for odd ΔJ transitions involving the $N_2(B)$ intermediate case wave functions arises from terms in Eq. (5) involving $V_{\rm diff}$.

Examination of Fig. 8 also reveals that the extent of fine-structure-changing collisions grows with increasing initial J. It is interesting to note that the populations in the F_2 and F_3 manifolds are comparable to the populations of final levels corresponding to fine-structure-conserving odd ΔJ inelastic collisions. As with the odd ΔJ transitions within the F_1 manifold, calculation of a sampling of the $A^{\,l}_{J'F'_i\epsilon',JF_i\epsilon}$ and $B^{\,l}_{J'F'_i\epsilon',JF_i\epsilon}$ coefficients in Eqs. (6a) and (6b) for these $F_1\rightarrow F_2,F_3$ transitions reveals that it is the V_{l2} terms in the interaction potential that enables these fine-structure-changing transitions. In the case (b) limit, the analysis in Sec. III shows that these fine-structure-changing transitions should have negligible probability. However, for the rotational levels of $N_2(B)$ under consideration ($J\leqslant 16$), the coupling scheme is still fairly close to case (a): For instance, the percentage $\Omega=0$ character for the $J=16$ F_1 levels is approximately 66%, while the case (a) and (b) limits are 100% and 25%, respectively.

Figures 9 and 10 show that fine-structure-changing transitions occur with almost the same probability as fine-structure-conserving ones for F_2 and F_3 initial levels. There is some evidence in Figs. 9(a) and 9(b) for an even–odd oscillation in the final state populations for $F_2\rightarrow F_2$ transitions for the $J=9$ and 10 F_2f initial levels, in analogy with the pronounced oscillations seen in Fig. 8 with F_1 levels. This small oscillation in the F_2 final state populations can be explained by the dependence on quantum numbers of the $3j$ symbol in the expression for $A^{\,l}_{J'F'_i\epsilon',JF_i\epsilon}$ in Eq. (6a). While this $3j$ symbol vanishes completely for $s=J'+l+J$ odd only when $\Omega=0$, its magnitude is depressed for odd vs even s when $\Omega>0$.[24,36] This oscillation decreases with increasing Ω and is hence more pronounced for $\Omega=1$ than for $\Omega=2$.

Pouilly and Alexander[15] predict that asymmetries in upward vs downward ΔJ transitions should be present within the F_2 manifold in the case (a) limit, as has already been observed in collisions of $^1\Pi$ molecules.[30–33] Such an asymmetry should, in principle, be observable in the final state populations displayed in Figs. 9(a) and 9(b) since they should be manifest oppositely for incident levels of the same e/f symmetry with J differing by one. While it is somewhat unfortunate that a complete distribution in the F_2 manifold could not be measured because of spectral overlap problems, nevertheless these asymmetries cannot be discerned in our experimental final state distributions. Perhaps the transition toward case (b) coupling in these $N_2(B)$ levels has reduced the expected magnitude of these predicted asymmetries.

Infinite-order-sudden (IOS) scaling relationships[28,34–37,46,47] have been used to interpret state-resolved

inelastic cross sections involving both intraelectronic[13,41,48] and interelectronic[12,13] transitions of open-shell molecules. As has been noted previously for $^2\Pi$ molecules,[28] an IOS factorization of the cross sections is possible only for case (a) coupling, wherein the fine-structure-conserving and -changing transitions each obey separate scaling relations. Since the IOS cross sections have an analogous quantum number dependence on angular momentum quantum numbers as the interaction potential, Eq. (5) shows that such a factorization for $^3\Pi$ molecules is also possible only at the case (a) limit. In this case, the fine-structure-conserving cross sections within the F_1 and F_3 manifolds can be written as

$$\sigma(J\Omega\epsilon\rightarrow J'\Omega\epsilon') = (2J'+1)\sum_l \frac{1}{2}[1+\epsilon\epsilon'(-1)^{J+J'+l}] \times \begin{pmatrix} J' & l & J \\ -\Omega & 0 & \Omega \end{pmatrix}^2 \sigma_l^0, \quad (14)$$

where the base cross sections σ_l^0 can be related to cross sections out of the $J=0$, $\Omega=0$ level. (Because of the interference[15] between V_{l0} and V_{l2} terms, such a factorization is not possible for the $\Omega=1$ manifold.)

Since N_2 is a homonuclear molecule, only the even l base cross sections in Eq. (14) will be nonzero here. This fact, along with the vanishing[24] of the $3j$ symbol in Eq. (14) for $\Omega=0$ and $J'+l+J$ odd, implies that odd ΔJ transitions will be forbidden by this scaling relation for $\Omega=0$, as Pouilly and Alexander[15] previously found for the potential coupling matrix elements. The occurrence of odd ΔJ transitions for $J>0$ F_1 initial levels can be reconciled with Eq. (14) by taking account of the intermediate case coupling [Eqs. (6a) and (6b)] of both initial and final levels. However, since the $J=0$ level can have no $\Omega=1$ or 2 admixture, no odd ΔJ transitions are allowed from $J=0$ in the IOS limit. Clearly, our experimental observation [Fig. 8(a)] of such transitions indicates that an IOS scaling analysis of our results is inappropriate.

C. Search for collisional transitions for the $W\,^3\Delta_u$ state

We also attempted to observe by the OODR technique nitrogen molecules which underwent collisional transitions from the $B\,^3\Pi_g$ state to the nearly isoenergetic[2,11] $W\,^3\Delta_u$ electronic state. Our goal was to obtain state-to-state information on $B\rightarrow W$ collisional interelectronic transitions, as we have done previously for the $A\rightarrow X$ transition in CN.[13] In order to maximize our detection sensitivity in this exploratory study, the pump laser was tuned to the P_1 B–A (3,0) bandhead in order to produce a large population of excited $N_2(B)$ molecules. From an analysis of their vibrationally and temporarily resolved observations of B–A emission upon pulsed laser excitation of the B state, Sadeghi and Setser[10] and Rotem and Rosenwaks[9(b)] estimate that the bimolecular rate constant for transfer from the $v_B=3$ to the $v_W=3$ manifold in $N_2(B)$–Ar collisions is greater than 10^{-11} molecule^{-1} cm^3 s^{-1}. This implies that at our operating pressure and a relatively long pump–probe delay of 200 ns typically approximately one-half of the initially produced B state molecules will have undergone a $B\rightarrow W$ collisional transition.

The only radiative transitions involving the $W\,^3\Delta_u$ state which have been previously identified[2,11] are the infrared B–W/W–B transition and the vacuum ultraviolet W–X transition. Neither of these is suitable for laser fluorescence detection of the W electronic state. This state, whose predominant electron configuration[2,7,49] is $\cdots 1\pi_u^3 3\sigma_g 1\pi_g^2$, has an allowed radiative transition to the higher lying $G\,^3\Delta_g$ state, whose electron configuration can be expressed as $\cdots 1\pi_u^2 3\sigma_g^2 1\pi_g^2$.[2,49] This latter state has only been observed spectroscopically through the Gaydon–Herman green $H\,^3\Phi_u$–$G\,^3\Delta_g$ band system.[50] As neither of these states has been connected to other states of molecular nitrogen, the electronic energy, and hence G–W transition frequency, is not precisely known. However, *ab initio* calculations[49] allow the G state electronic energy to be estimated with reasonable confidence. We have calculated Franck–Condon factors for the G–W bands by the RKR method with parameters derived in spectroscopic analyses of the B–W[11] and H–G[50] band systems.

Since the equilibrium internuclear separations are widely different for the W and G states (1.28 vs 1.61 Å, respectively), the Franck–Condon array is strongly off-diagonal. Carroll *et al.*[50] surmised that the G–W system may not have previously been observed because, apart from possible difficulties in populating the G state, the strongest bands are predicted to fall in the red or near infrared, where these would be obscured by the strong B–A first positive system.[2–4] We have attempted to detect the W state by probe laser fluorescence excitation in the near ultraviolet; the Franck–Condon factors calculated for transitions in this wavelength range from $v_W=3$ to $v_G=3$ to 5 range from 0.05 to 0.07. (We have been able to detect CN B–X and B–A bands with Franck–Condon factors of this magnitude.[13]) A red-cutoff filter and a blue-cutoff filter were placed in front of the photomultiplier to pass G–W fluorescence in the region from 400 to 600 nm and to block laser scattered light and B–A pump laser excited fluorescence.

No G–W probe laser fluorescence signal could be detected, despite scanning the probe laser from 375 to 400 nm. Our detection sensitivity was sufficiently large that we would have been able to observe G–W OODR signals a factor of 10 smaller than those observed for the C–B band. The scanned region was more than 1500 cm^{-1}, which is approximately the G state vibrational spacing.[50] In this way, we would have been able to excite some G–W band even if the calculated G state electronic energy were slightly incorrect.

A careful analysis[51] of the G state electronic wave function and G–W transition moment suggests that, in fact, the oscillator strength of this band is quite small. The G state is actually a virtually equal mixture of electronic configurations corresponding to either the $1\pi_u$ pair or the $1\pi_g$ pair being triplet coupled (with the other pair being singlet coupled). The contribution of these configurations to the G–W transition moment have opposite sign and approximately cancel.

V. DISCUSSION AND CONCLUSION

In this paper, we have presented relative state-to-state cross sections for rotationally inelastic collisions of

$N_2(B\,^3\Pi_g)$ with Ar. Final state populations were determined for incident levels in all three fine-structure manifolds. A pronounced preference for conservation of fine-structure label with even ΔJ changes was observed for incident F_1 levels. This result is consistent with a propensity rule derived by Pouilly and Alexander[15] for inelastic collisions of homonuclear $^3\Pi$ molecules with Hund's case (a) coupling. The experimentally observed propensity was found to be very strong for initial $J = 0$ but decreased monotonically with increasing J. For incident levels in the F_2 and F_3 spin–orbit manifolds, fine-structure-changing collisional transitions were found to occur with a probability essentially equal to that for fine-structure-conserving transitions. A residual even–odd alternation in the F_2 final state populations was observed for incident F_2 levels.

These experimental results have been interpreted in terms of the quantum scattering theory for a $^3\Pi$ molecule with coupling between Hund's cases (a) and (b). As discussed in detail in Sec. III, two potential energy surfaces are required for a description of the interaction of a $^3\Pi$ molecule with a structureless target. Our experimental results show, in particular for $N_2(B)$–Ar collisions, that the difference potential $V_{\rm diff}$ is not insignificant compared to the sum potential $V_{\rm sum}$. This in turn implies that there is a significant variation in the interaction between a nitrogen molecule in the B state and an argon atom when the unfilled π electron is in vs perpendicular to the triatomic molecular scattering plane. The predominant electron configuration for $N_2(B)$ is $\cdots 1\pi_u^4 3\sigma_g 1\pi_g$.[2,7,49] Thus, the alignment of the $1\pi_g$ electron, which corresponds roughly to an antibonding $2p\pi$ orbital, has a significant effect on the $N_2(B)$–Ar interaction. Because of its antibonding nature and lower ionization potential,[2] this orbital would be expected to be somewhat diffuse and to extend out beyond the more tightly bound $1\pi_u$ and $3\sigma_g$ orbitals.

It is interesting to compare these inferences on the $N_2(B)$–Ar system with what is known about $NO(X\,^2\Pi)$–Ar collisions. The ground state $NO(X)$ electron configuration differs from that for $N_2(B)$ only in the addition of another electron to fill the open σ orbital. Both experimental crossed beam studies[52] and quantum scattering calculations[53] show that fine-structure-changing collisional transitions are approximately an order of magnitude less probable than those in which the fine-structure label is conserved. In the nearly pure case (a) coupling appropriate for $NO(X)$, the probability of fine-structure-changing transitions is related to the magnitude of the difference potential $V_{\rm diff}$. This behavior arises because, for the $NO(X)$–Ar system, the interaction potential only very weakly depends on the orientation of the unfilled π orbital with respect to the triatomic plane, as has been concluded from an electron-gas calculation of the $NO(X)$–Ar A' and A'' potential energy surfaces.[54] This suggests that for the $NO(X)$–Ar system the filled orbitals shield the incoming perturber atom from interacting strongly with this unfilled π orbital. This orbital would be expected to be somewhat more diffuse in $N_2(B)$ vs $NO(X)$ because of a slightly lower ionization potential (8.2 vs 9.3 eV[55]). It would be interesting to compare our qualitative conclusions about the $N_2(B)$–Ar interaction potential, and the comparison with $NO(X)$–Ar, with actual *ab initio* computations of these potential energy surfaces.

We have also described an unsuccessful attempt to detect the $W\,^3\Delta_u$ state by visible or near ultraviolet laser fluorescence excitation in the hitherto unobserved G–W band system. At present, there is no convenient and sensitive means for detection of this N_2 electronic state, which clearly plays a significant role in environments containing electronically excited triplet state molecules. There clearly is a challenge to devise other detection schemes for this important low-lying electronic state of molecular nitrogen.

ACKNOWLEDGMENTS

The authors are greatly indebted to Millard Alexander for his encouragement and numerous conversations on the quantum collision theory for open-shell molecules. His and H.-J. Werner's assistance in estimating the N_2 G–W transition moment is also greatly appreciated. This research was supported by the National Science Foundation under Grant No. CHE-8705912.

[1] J. H. Kolts and D. W. Setser, in *Reactive Intermediates in the Gas Phase*, edited by D. W. Setser (Academic, New York, 1979), p. 151.
[2] A. Lofthus and P. H. Krupenie, J. Phys. Chem. Ref. Data **6**, 113 (1977).
[3] G. H. Dieke and D. F. Heath, Johns Hopkins Spectroscopic Report No. 17, Department of Physics, The Johns Hopkins University, Baltimore, MD (1959).
[4] F. Roux, F. Michaud, and J. Verges, J. Mol. Spectrosc. **97**, 253 (1983); **104**, 420 (1984).
[5] T. A. Carlson, N. Duric, P. Erman, and M. Larsson, Phys. Scr. **19**, 25 (1979).
[6] E. Eyler and F. M. Pipkin, J. Chem. Phys. **79**, 3654 (1983).
[7] H.-J. Werner, J. Kalcher, and E.-A. Reinsch, J. Chem. Phys. **81**, 2420 (1984).
[8] R. F. Heidner, D. G. Sutton, and S. N. Suchard, Chem. Phys. Lett. **37**, 243 (1976).
[9] (a) A. Rotem, I. Nadler, and S. Rosenwaks, Chem. Phys. Lett. **83**, 281 (1981); (b) A. Rotem and S. Rosenwaks, Opt. Eng. **22**, 564 (1983); (c) A. Rotem, I. Nadler, and S. Rosenwaks, J. Chem. Phys. **76**, 2109 (1982); (d) I. Nadler and S. Rosenwaks, *ibid.* **83**, 3932 (1985).
[10] N. Sadeghi and D. W. Setser, Chem. Phys. Lett. **77**, 308 (1981); J. Chem. Phys. **79**, 2710 (1983).
[11] D. Cerny, F. Roux, C. Effantin, J. d'Incan, and J. Verges, J. Mol. Spectrosc. **81**, 216 (1980).
[12] D. H. Katayama, J. Chem. Phys. **81**, 3495 (1984); Phys. Rev. Lett. **54**, 657 (1985); D. H. Katayama and A. V. Dentamaro, J. Chem. Phys. **85**, 2595 (1986).
[13] N. Furio, A. Ali, and P. J. Dagdigian, J. Chem. Phys. **85**, 3860 (1986); G. Jihua, A. Ali, and P. J. Dagdigian, *ibid.* **85**, 7098 (1986); A. Ali, G. Jihua, and P. J. Dagdigian, *ibid.* **87**, 2045 (1987).
[14] D. H. Katayama, J. Chem. Phys. **84**, 1477 (1986).
[15] B. Pouilly and M. H. Alexander, J. Chem. Phys. **79**, 1545 (1983).
[16] N. Sadeghi and D. W. Setser, Chem. Phys. Lett. **82**, 44 (1981).
[17] G. Herzberg, *Molecular Spectra and Molecular Structure. I. Spectra of Diatomic Molecules* (Van Nostrand, Princeton, 1950).
[18] J. T. Hougen, Natl. Bur. Stand. (U.S.) Monogr. **115** (1970).
[19] R. N. Zare, A. L. Schmeltekopf, W. J. Harrop, and D. L. Albritton, J. Mol. Spectrosc. **46**, 37 (1973).
[20] H. Lefebvre-Brion and R. W. Field, *Perturbations in the Spectra of Diatomic Molecules* (Academic, New York, 1986).
[21] M. Larsson, Phys. Scr. **23**, 835 (1981).
[22] J. M. Brown, J. T. Hougen, K. P. Huber, J. W. C. Johns, I. Kopp, H. Lefebvre-Brion, A. J. Merer, D. A. Ramsay, J. Rostas, and R. N. Zare, J. Mol. Spectrosc. **55**, 500 (1975).
[23] J. M. Brown and B. J. Howard, Mol. Phys. **31**, 1517; **32**, 1197 (1976).
[24] D. M. Brink and G. R. Satchler, *Angular Momentum*, 2nd ed. (Clarendon, Oxford, 1968).

[25]M. H. Alexander and P. J. Dagdigian, J. Chem. Phys. **80**, 4325 (1984).
[26]B. Pouilly, P. J. Dagdigian, and M. H. Alexander, J. Chem. Phys. (in press).
[27]M. H. Alexander, Chem. Phys. **92**, 337 (1985).
[28]M. H. Alexander, J. Chem. Phys. **76**, 5974 (1982).
[29]D. Secrest, in *Atom–Molecule Collision Theory: A Guide for the Experimentalist*, edited by R. B. Bernstein (Plenum, New York, 1979), p. 301.
[30]Ch. Ottinger, R. Velasco, and R. N. Zare, J. Chem. Phys. **52**, 1636 (1970).
[31]K. Bergmann and W. Demtröder, J. Phys. B **5**, 1386, 2098 (1972).
[32]D. Poppe, Chem. Phys. Lett. **19**, 63 (1973).
[33]D. Lemoine, G. C. Corey, M. H. Alexander, and J. Derouard, Chem. Phys. (in press).
[34]M. H. Alexander, J. Chem. Phys. **76**, 3637 (1982).
[35]M. H. Alexander and S. L. Davis, J. Chem. Phys. **79**, 227 (1983).
[36]M. H. Alexander and P. J. Dagdigian, J. Chem. Phys. **79**, 302 (1983).
[37]M. H. Alexander and G. C. Corey, J. Chem. Phys. **84**, 100 (1986).
[38]K. Takayanagi, Adv. At. Mol. Phys. **1**, 149 (1965).
[39]Reference 24, p. 137.
[40]G. C. Corey and F. R. McCourt, J. Phys. Chem. **87**, 2723 (1983).
[41]P. J. Dagdigian and S. J. Bullman, J. Chem. Phys. **82**, 1341 (1985); M. H. Alexander, S. L. Davis, and P. J. Dagdigian, *ibid.* **83**, 556 (1985).
[42]R. K. Lengel and D. R. Crosley, J. Chem. Phys. **67**, 2085 (1977).
[43]G. C. Corey and M. H. Alexander, J. Chem. Phys. **83**, 5060 (1985).
[44]G. C. Corey, M. H. Alexander, and P. J. Dagdigian, J. Chem. Phys. **84**, 1547 (1986).
[45]C. H. Greene and R. N. Zare, J. Chem. Phys. **78**, 6741 (1983).
[46]R. Goldflam, S. Green, and D. J. Kouri, J. Chem. Phys. **67**, 4149 (1977); R. Goldflam, D. J. Kouri, and S. Green, *ibid.* **67**, 5661 (1977).
[47]V. Khare, J. Chem. Phys. **68**, 4631 (1978).
[48]C. Dufour, B. Pinchemel, M. Douay, J. Schamps, and M. H. Alexander, Chem. Phys. **98**, 315 (1985).
[49]H. H. Michels, Adv. Chem. Phys. **45**, 225 (1981).
[50]P. K. Carroll, C. C. Collins, and J. T. Murnaghan, J. Phys. B **5**, 1634 (1972).
[51]M. H. Alexander and H.-J. Werner (unpublished).
[52]P. Andresen, H. Joswig, H. Pauly, and R. Schinke, J. Chem. Phys. **77**, 2204 (1982); H. Joswig, P. Andresen, and R. Schinke, *ibid.* **85**, 1904 (1986).
[53]T. Orlikowski and M. H. Alexander, J. Chem. Phys. **79**, 6006 (1983); **80**, 4133 (1984); M. H. Alexander and T. Orlikowski, *ibid.* **80**, 1506 (1984); G. C. Corey and M. H. Alexander, *ibid.* **85**, 5652 (1986).
[54]G. C. Nielson, G. A. Parker, and R. T Pack, J. Chem. Phys. **66**, 1396 (1977).
[55]K. P. Huber and G. Herzberg, *Molecular Spectra and Molecular Structure. IV. Constants of Diatomic Molecules* (Van Nostrand Reinhold, New York, 1979).